Review article

Ana M.R. Pinto* and Manuel Lopez-Amo

All-fiber lasers through photonic crystal fibers

Abstract: A review on all-fiber lasers based on photonic crystal fibers is presented. Photonic crystal fibers present improved features beyond what conventional optical fibers can offer. Due to their geometric versatility, photonic crystal fibers can present special properties and abilities which can lead to enhanced lasing structures. A brief description of photonic crystal fibers and fiber laser's properties is presented. All-fiber laser structures developed using photonic crystal fibers are described and divided in two groups, depending on the cavity topology: ring cavity fiber lasers and linear cavity fiber lasers. All-fiber lasers applications in the photonic crystal fiber related sensing field are described.

Keywords: fiber laser; photonic crystal fiber; microstructured fiber; laser; optical fiber.

***Corresponding author: Ana M.R. Pinto,** Department of Electric and Electronic Engineering, Universidad Pública de Navarra, 31006 Pamplona, Spain, Phone: +34-94816044, Fax: +34-948169720, e-mail: anamargarida.rodrigues@unavarra.es
Manuel Lopez-Amo: Department of Electric and Electronic Engineering, Universidad Pública de Navarra, 31006 Pamplona, Spain

Edited by Alan Willner

1 Introduction

Fiber lasers development had a huge impact in fields such as medicine, sensing, communications and materials processing. Despite the fact that the first fiber laser was only developed in 1964, its history can be traced back to the end of the nineteen century. In 1900, Max Planck provided the world with the understanding that light is a form of electromagnetic radiation, followed by Albert Einstein's theory of light emission and stimulated emission concept in 1916. It took almost 40 years for scientists and engineers to apply these principles to practical purposes, but it finally happened in the 1950s with the conception of the idea of the maser (microwave amplification by stimulated emission radiation), a device that amplified microwaves. The maser was demonstrated in 1954 at Columbia University, radiating at a wavelength of a little more than 1 cm and generating approximately 10 nW of power [1]. This development awakened scientists to the idea of using the same principle in the optical region. The first detailed written proposal of this "optical maser" was published in December 1958 [2], now known to all as laser (light amplification by stimulated emission radiation). In 1960 the first laser was experimentally demonstrated using a synthetic ruby with its ends silver-coated, serving as a Fabry-Perot resonator, pumped by photographic flash lamps [3]. By this time, a race was already on to build lasers, and as so, in the following years there was a burst of different lasers: uranium laser, helium-neon laser, neodymium glass laser, gallium-arsenide laser, yttrium aluminum garnet laser, etc. [4].

Optical fiber waveguides development revolutionized several fields such as telecommunications and sensing, leading to the creation of high sensitivity and controlled systems based on light guidance. Optical fibers present small size, robustness, flexibility and the aptitude to be used even in the presence of unfavorable environmental conditions (such as noise, strong electromagnetic fields, explosive or chemically corrosive media). After a groundwork study of the first few low-order modes in the visible region of the spectrum [5], optical fibers were proposed for the first time as cavities for lasers [6], showing that the principal advantages for maser applications were the mode selection and the stronger mode coupling. However, it was only in 1964 that the first fiber laser was demonstrated [7], using 1 m neodymium glass core fiber in a spring-shaped coil slipped around a linear flashlamp. It took more than two decades before fiber laser technology came into its own. After 1985, several groups started to try doping fiber cores with rare-earth elements to make fiber lasers [8, 9], obtaining very attractive results which lead to a nonstop of research on the area. Nowadays, all-fiber laser structures can provide good performances with minimal sensitivity to environmental disturbances as well as high reliability since the all-fiber system may not be as easily misaligned as a bulk system might.

Standard optical fibers (OFs) present an excellent performance in fiber optic telecommunications. Despite

of that, the intrinsic properties of silica have imposed restrictions in the evolution of this technology. An evident restriction is the material selection for the core and cladding in order to have matching thermal, chemical and optical properties; other limitations are related to its geometry and refractive index profile, which does not allow freely engineering fiber optic characteristics such as inherent losses, dispersion, nonlinearity and birefringence [10]. These limitations and restrictions lead to the appearance of photonic crystal fibers (PCFs) in 1996. PCFs present unprecedented properties, been able to overcome many of standard optical fibers limitations. Photonic crystal fibers geometry is characterized by a periodic arrangement of air-holes running along the entire length of the fiber, centered on a solid or hollow-core. The major difference between both kinds of fibers relies on the fact that the waveguide properties of photonic crystal fibers are not due to spatially varying glass composition as in conventional fibers, but from an arrangement of very tiny and closely spaced air-holes which go through the whole fiber length. In contrast with standard optical fibers, photonic crystal fibers can be made of a single material and have several geometric parameters that can be manipulated offering great flexibility of design [11, 12]. Consequently, there is a high interest in employing photonic crystal fibers technology in all kinds of fields.

In this paper, a review of all-fiber lasers developed using photonic crystal fibers is presented. Photonic crystal fiber's main properties are presented in Section 2. In Section 3, the fiber laser's principles and properties are described. In Section 4 and 5, ring cavity and linear cavity fiber lasers are disclosed, respectively. Developed sensing applications using all-fiber lasers are introduced in Section 6. And, at last, Section 7 presents the conclusions to the present manuscript.

2 Photonic crystal fibers main properties

The first PCF was materialized in November of 1995: a structure in the form of a silica fiber with a regular hexagonal pattern of air-holes running its entire length. This PCF had the light strongly confined in the solid silica core region, and its light guidance mechanism lie in modified total internal reflection [10]. This exceptional structure first analysis showed means to provide enhanced interaction between light and gas (in the air-holes) in order to be used as gas sensor or to study non linear effects [13]. Following this development, the field of photonic crystal fibers became extremely popular and numerous research groups all around the world started making research in this area. With photonic crystal fibers almost everything seemed feasible: having single mode guidance at all wavelengths [14]; controlling the dispersion with unprecedented freedom, from having zero dispersion at visible wavelengths to having large normal dispersion at the third telecommunications window, while maintaining single mode operation [15, 16]; obtaining extremely high values of birefringence with high temperature insensitivity [17]; guiding in a hollow-core through photonic band gap guidance [18] or broad optical transmission bands covering the visible and near-IR of the electromagnetic spectrum [19], and even overcoming limitations inherent to interactions between light and matter and enhancing gas based non-linear effects [20].

The geometry of common optical fibers normally entails a doped silica solid-core surrounded by a pure silica solid-cladding, ensuring that the core refractive index is higher than the one of the cladding. Photonic crystal fiber's geometry is characterized by a microstructured air-hole cladding running along the entire length of the fiber, which surrounds the core that can be solid or hollow. During modeling as well as the manufacturing process there are different physical parameters to be controlled: the core diameter -ρ- (which for solid-core PCF is defined as the diameter of the ring formed by the innermost air-holes), the diameter of the air-holes in the cladding -d- and the pitch -Λ- (distance between the centers of two consecutive air-holes). These parameters are typically of the order of micrometers, for example, the first PCF ever fabricated presented ρ=4.6 μm, Λ=2.3 μm and 0.2 μm<d<1.2 μm [13]. A huge advantage of PCF's geometry is the ability to fabricate them with a single material and still insure guidance in the core, solid or hollow, allowing the fabrication of fibers without doping materials. PCFs can be divided in two families based on their geometry: solid-core and hollow-core PCFs.

2.1 Solid-core photonic crystal fibers

Solid-core PCFs cross section presents a periodic array of air holes surrounding a solid-core, which are extended invariantly along the fiber length. When using a single material in the fiber manufacturing, this cross sectional configuration leads to a lowering of the cladding's effective refractive index given that the solid-core is made of the same material, allowing the light guidance mechanism to be total internal reflection.

In solid-core PCFs, core refractive index is greater than the average index of the cladding, consequently the

fiber can guide via total internal reflection, as an ordinary OF does. This means that there are propagation constants, β, available to light in the core but not to light propagating in the cladding:

$$\beta_{FSM}<\beta<kn_{co} \quad (1)$$

where β_{FSM} is the propagation constant of the fundamental space-filling mode, $k=2\pi/\lambda$ is the wavenumber and n_{co} is the refractive index of the material of the core (typically silica). FSM is defined as the fundamental mode of the infinite photonic crystal cladding if the core is absent; as a result β_{FSM} represents the maximum β allowed in the cladding. The lower limit for β in a step-index fiber is kn_{cl}, in the same way for a PCF:

$$\beta_{FSM}=kn_{cl}(\text{PCF}) \quad (2)$$

where n_{cl}(PCF) is the effective refractive index of the PCF cladding.

Another outstanding property of these fibers is their ability to present endlessly single mode guidance. In solid-core PCFs, the TIR guidance mechanism depends on the nature of the core and the air-hole arrangement, which will lead to an unusual interaction of the guided mode with the photonic crystal cladding. This unusual interaction allows monomode wave guidance possible over most of the transmission window of silica, which is a feature that appears to be unique to this type of structure. As so, it is always possible to tailor d/Λ in order to obtain single mode guidance in a PCF [14, 21].

An illustration of a highly birefringent (Hi-Bi) solid-core PCF cross section structure is presented in Figure 1(A), as well as its simulated fundamental mode in Figure 1(B) (using BandSolve from Rsoft Design Group, Inc., New York, USA).

Solid-core PCFs improved features over conventional OFs lead to an increasing number of applications in diverse areas of technology and science. Supercontinuum sources based in PCFs can be applied in optical coherence tomography [22] and in spectroscopy [23]. PCFs for sensing applications have also been widely demonstrated [24], in order to measure a variety of parameters: curvature [25]; strain/displacement [26]; electric field [27] as well as magnetic field [28]; pressure [29]; temperature [30]; torsion [31] and transversal load [32]; refractive index [33]; vibration [34]; gases [35]; DNA [36]; proteins [37]; rhodamine [38]; salinity [39]; pH [40] and humidity [41].

2.2 Hollow-core photonic crystal fibers

Hollow-core photonic crystal fibers present a microstructured air-hole cladding, which surrounds a hollow-core. This hollow-core in the middle of the microstructured cladding leads to a negative core-cladding refractive index difference, and as so the PCF cannot operate via total internal reflection. However, an appropriately designed holey photonic crystal cladding, running along the entire length of the fiber, can prevent the light to escape from the hollow-core. Under these circumstances, waveguiding is only possible if a photonic bandgap exists. The first band gap guiding PCF was reported in 1999 [18], demonstrating light confinement and guidance in an air-core PCF only at certain wavelength bands, corresponding to the presence of a full 2D band gap in the photonic crystal cladding. Figure 2(A) presents the illustration of a hollow-core PCF's cross section and Figure 2(B) the simulated fundamental mode falling inside the bandgap (using BandSolve from Rsoft).

In 2D crystal structures, photonic bandgaps exist and prevent propagation of light within a certain range of frequencies. If the periodicity of the structure is broken with a defect, a special region with different optical properties can be created. The defect region can support modes with frequencies falling inside the photonic bandgap, but

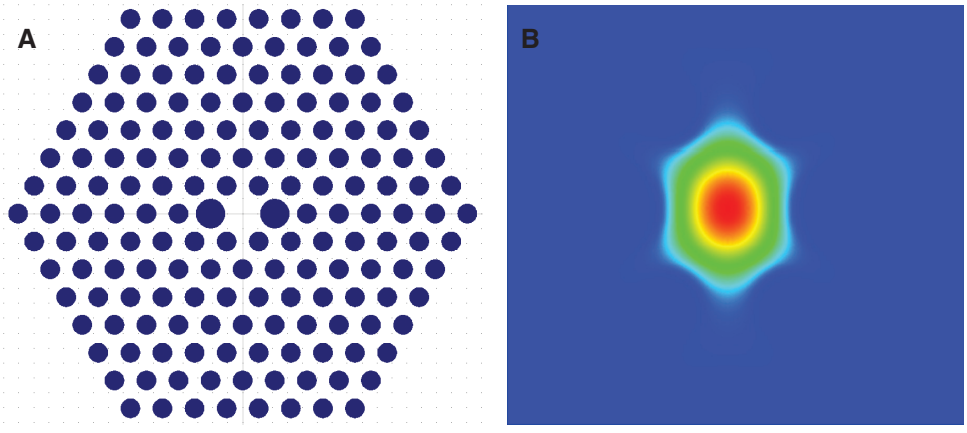

Figure 1 (A) Illustration of a Hi-Bi PCF's cross section (colors: blue-air, white-silica) and (B) fiber's fundamental mode (at 1550 nm).

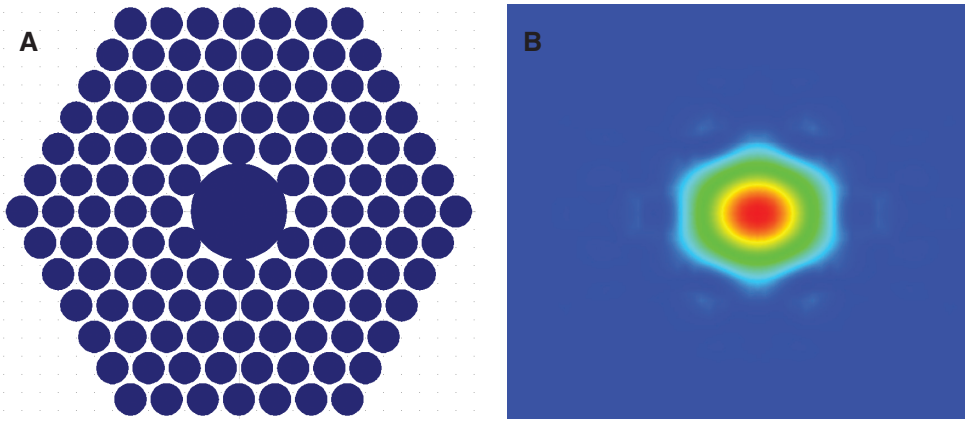

Figure 2 (A) Illustration of a hollow-core PCF's cross section (colors: blue-air, white-silica) and (B) fiber's fundamental mode in the band gap (at 1550 nm).

since around this defect there is a photonic bandgap, light within the defect will remain confined in the vicinity of the defect [42]. This effect is illustrated in Figure 3: suppose a hollow-core PCF is designed to work in the red visible region of the electromagnetic spectrum. When the PCF is illuminated by a blue LED, all light will be refracted and no light will be guided by the fiber, consequently no light will come out at the end of the PCF. On the other hand, if the PCF is illuminated by a broadband source the red component of light will be guided appearing at the fiber end and all other frequency components of light (like green or yellow light, represented in Figure 3 for illustrative purposes) will be refracted.

From the illustration on Figure 3 it can be deducted that modes falling outside the defect will be refracted, while modes falling inside the defect region will be strongly confined to the defect and guided along it throughout the entire length of the fiber. When using a simulation engine to discover the band structures of a hollow-core PCF, such as the depicted in Figure 2(A), one finds that this band structure exhibits a significant gap, represented in Figure 4(A) by the squared filled area at $2\pi a/\lambda=9.05$. When generating the map of the band gaps, to see what is happening in that squared area, we find two gaps that vary in width and starting position. Figure 4(B) shows these band gaps as well as the light line (gray line). The modes guided in the gaps can be found near the intersection between the gaps and the light line, which for this fiber seems to be for $8.8<\beta<9.4$.

This guidance mechanism allows light to be guided in air, not possible with standard OFs (for which positive core-cladding refractive index difference is imperative). Moreover, it presents noteworthy advantages like less interaction between guided light and material forming the fiber, therefore increasing threshold powers for lasing based in nonlinear effects, allowing high power transmission [18]; the ability to fill the core of the fiber with gases and liquids leading to study gas-based nonlinear optics [20], optical tweezers propulsion and particle guidance in liquids [43] and even photochemical reactions [44]; filtering away unwanted wavelengths since this fiber only works in a precise range of wavelengths, and thus allowing applications like selective sensing of antibodies [45] and gases detection [46]; and extremely small Fresnel reflections, since the refractive index discontinuity

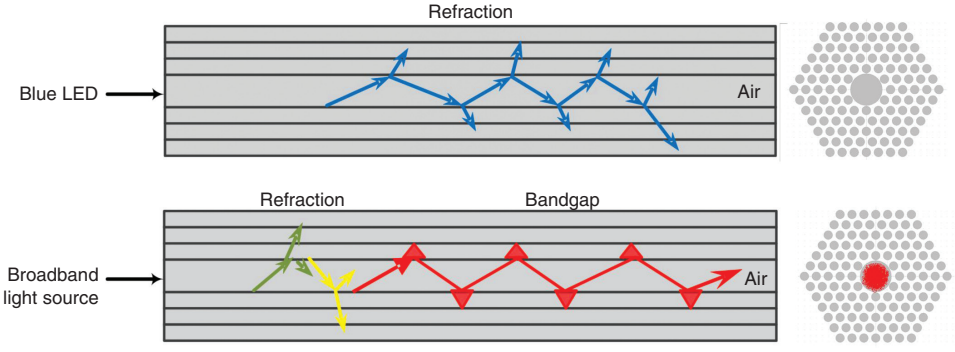

Figure 3 Illustration of the photonic bandgap guidance mechanism in a hollow-core PCF.

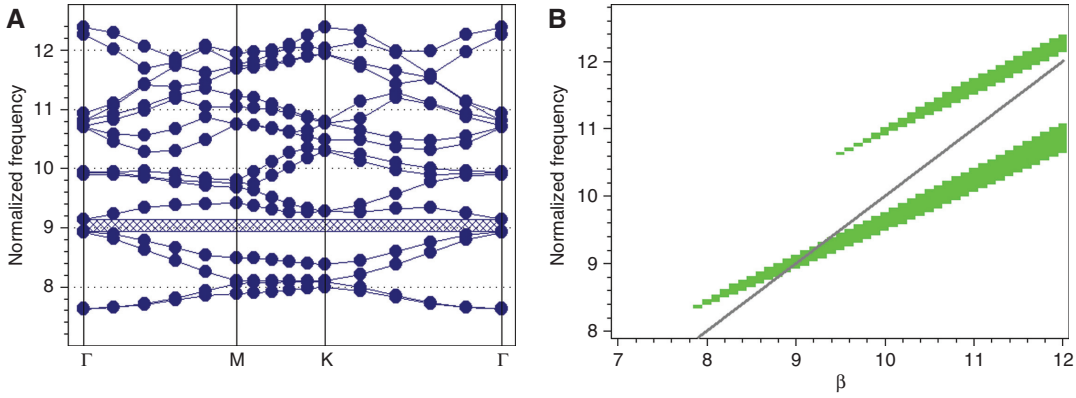

Figure 4 (A) Band structure for a hollow-core PCF and (B) Gap map as a function of the propagation constant β; Γ,M,K are the points of interest in the Brillouin Zone.

between the outside world and the fiber mode can be very tiny, leading to the possibility of using these fibers as displacement sensors [47].

3 Fiber lasers principles and properties

Since the development of the first fiber laser in the 1960s, the scientific community started to demonstrate a lot of interest in possible applications. Areas such as material processing, spectroscopy, medicine, sensing and telecommunications are potential application fields for this kind of laser. Basic laser schematic generally entails a gain medium to provide amplification and an optical cavity to trap the light, creating a positive feedback. Lasing occurs when the total gain in the cavity is larger than the total losses. In fiber lasers, the gain medium is an optical fiber and there are three types of laser cavities depending on the topology: linear, ring and random. The two first laser cavities will be explained in detailed further later in this manuscript, as they are the most common and important. Random cavities in all-fiber lasers are very recent, and as so will be considered in this manuscript as part of linear cavity lasers. Random lasers do not have physical cavities, they present what are called open cavities and are said to be "mirror-less" or to present distributed mirrors. Random lasers characteristic output is defined by multiple scattering and not by the laser cavity. The multiple scattering of photons in the amplifying medium increases the effective optical path, resulting in lasing [48]. By using the intrinsic disorder of an optical fiber, a random laser can be obtained. The refractive index of optical fibers has submicron scale inhomogeneities that are randomly distributed along the fiber. During propagation, the light will be scattered by these inhomogeneities obeying the Rayleigh's law [49]. Taking advantage of these Rayleigh scattering events as an active part in the laser, this is saying as a distributed/random mirror in the laser cavity, can lead to the enhancement of the laser's performance in three distinct ways: using the distributed random mirrors together with physical reflectors (in conventional resonant cavity) to enhance laser performance (Figure 5A); using distributed mirrors with only one reflector, thus reducing the need for two mirrors (Figure 5B); or even by not using physical reflectors at all, having then an all-fiber totally random fiber laser (Figure 5C).

Laser cavities are designed using reflectors. There is a variety of reflectors that can be used in all-fiber lasers. A very common all-fiber laser reflector is the fiber loop mirror (FLM), due to its low sensitivity to environmental noise. These reflectors are designed forming a loop by fusion splicing the output ports of a directional coupler, resulting in low-loss and stable devices. The input light entering the optical coupler will be divided in two waves that travel with identical optical paths in opposite directions and interfere when reentering the coupler, as illustrated in Figure 6. It was shown that the variation of reflectivity with wavelength and fiber birefringence of a perfect device (disregarding the losses of splice, fiber and optical coupler) can be adjusted from 0 to 100% by controlling the birefringence of the fiber loop [50]. If the fiber loop mirror is constituted only by a fiber with no birefringence (or negligible birefringence, as in the case of common telecommunications single mode fiber) it will act as a perfect mirror: the light is reflected back into the input port while, due to the energy conservation, no light is transmitted to the output port. When there is birefringence in the loop, the two counter propagating waves will travel trough the optical path with different velocities, due to the birefringence of the fiber. After propagating around the loop, the difference in the propagating wave's velocities will lead

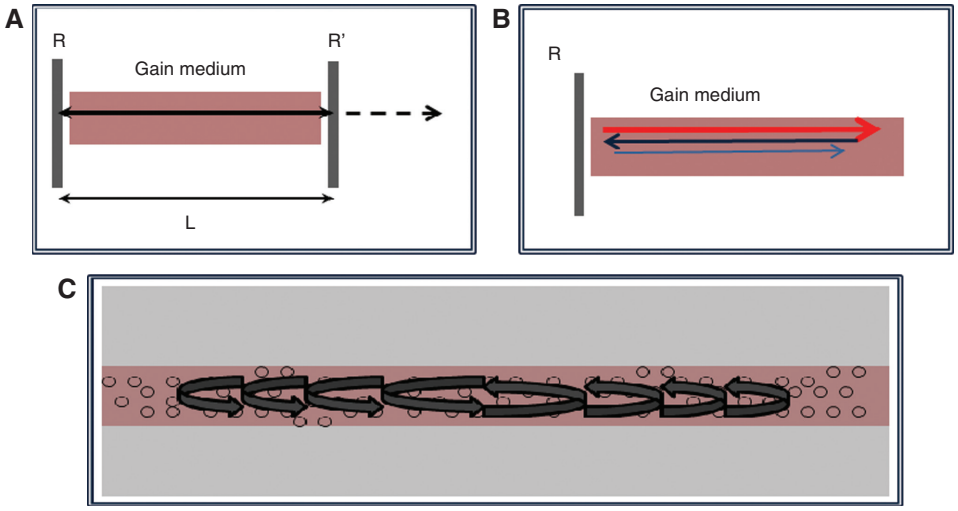

Figure 5 Illustration of three different laser cavities: (A) conventional resonant cavity, (B) one reflector cavity and (C) random cavity.

to a variable interference term in the output port (transmission and reflection). The wavelength spacing between two consecutive interference channels in the output spectrum is given by $\Delta\lambda=\lambda^2/BL$, where B and L are the birefringence and length of the fiber, respectively. Fiber loop mirrors that exploit nonlinear phase shift of optical fibers are usually addressed as Sagnac interferometers [50, 51].

Another familiar type of laser reflector in all-fiber lasers is the Fabry-Perot interferometer (FPI), which consists of two mirrors of reflectance R_1 and R_2 separated by a cavity of length *d*. A light beam entering the cavity is reflected multiple times between the reflectors. Each beam has a fixed phase difference with respect to the preceding one; this phase difference corresponds to the extra path length travelled in the cavity. The FPI output signal is a periodic function with a period given by $\Delta\lambda_{FPI}=\lambda^2/2nd$. There are also other interferometers that can be used as laser reflectors, such as Modal and Mach-Zehnder interferometers, but are not as commonly used.

Another approach to design the fiber cavity is using gratings. Different kinds of gratings can be used, for example: fiber Bragg grating (FBG), which couples the forward propagating core mode to the backward propagating core mode; long-period fiber grating (LPG) that can couple the forward propagating core mode to one or a few of the forward propagating cladding modes; chirped fiber grating, that has a wider reflection spectrum and each wavelength component is reflected at different positions, which results in a delay time difference for different reflected wavelengths; tilted fiber grating can couple the forward propagating core mode to the backward propagating core mode and a backward propagating cladding mode; sampled fiber grating, can reflect several wavelength components with equal wavelength spacing; etc. Among all of them, the FBGs are the most widely used in laser cavities. In FBGs the Bragg wavelength ,the wavelength at which the light that is reflected, is given by $\lambda_{Bragg}=2.n_{eff}.\Lambda$, where n_{eff} is the effective refractive index of the fiber core and Λ is the grating period.

The state-of-the-art of ring and linear cavities will be presented in the following sections, in the order depicted in the Figure 7.

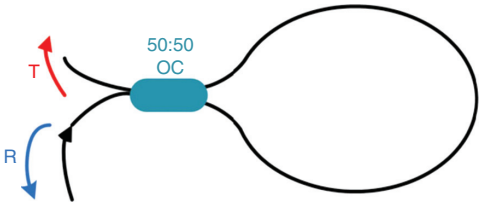

Figure 6 Fiber loop mirror configuration.

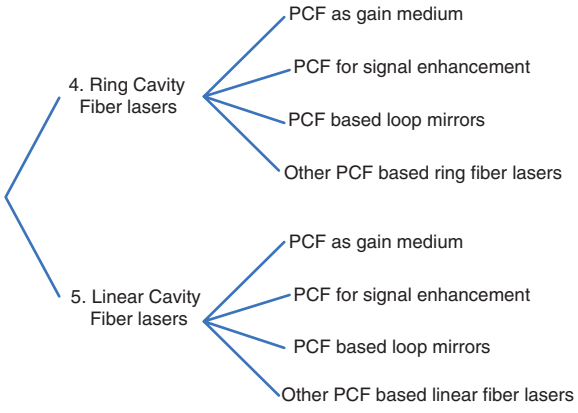

Figure 7 Diagram of the following sections disclosing the all-fiber lasers developed.

4 Ring cavity fiber lasers

Ring cavity fiber lasers have excellent lasing efficiency and are able to eliminate back scattering, been often used to realize unidirectional operation. The simplest conventional fiber ring laser structure entails two ports of a optical coupler connected together to form the ring cavity and an isolator (ISO) to insure unidirectional operation, as in Figure 8.

In this section, the state-of-the-art of the developed ring cavity fiber lasers will be presented. Section 4.1 provides the description of the ring fiber lasers using PCF as gain media. In Section 4.2 the fiber lasers using PCFs for signal enhancement are presented, Section 4.3 describes the fiber lasers developed based in PCF loop mirrors and Section 4.4 presents other PCF based ring fiber lasers.

4.1 PCF as gain medium

Quite numerous authors have used photonic crystal fibers as gain media in ring cavity fiber lasers. Multiwavelength erbium-doped ring fiber lasers were developed: by using a highly nonlinear PCF in combination with a fiber loop mirror [52]; or through three FBGs and a highly nonlinear PCF, reaching stability and uniformity based on four-wave-mixing [53]; or by employing a multimode FBG and a highly nonlinear PCF to induce four-wave-mixing effect [54]; or making use of a side-leakage PCF based filter incorporated into the ring cavity [55]; or based on four-wave-mixing in a length of high nonlinear PCF and a sampled fiber grating [56]; or even by exploiting a erbium-doped PCF and inducing nonlinear polarization rotation [57]. A dual-wavelength erbium-doped ring fiber laser was developed based on FBGs and a highly PCF [58]. A four-wavelength erbium-doped fiber laser was accomplished through four-wave-mixing using a highly nonlinear PCF and two FBGs [59]. Also, by using a highly nonlinear PCF in a ring cavity, the multiple mode instabilities in an erbium-doped fiber laser were suppressed [60]. A highly efficient erbium-doped fiber laser was obtained using home-made PCFs and a tunable filter [61]. Some authors develop multiwavelength Brillouin fiber ring lasers: by using a piece of 100 m long pure silica solid-core PCF [62] or through a 3 m long chalcogenide photonic crystal fiber [63]. And even ytterbium fiber ring lasers were generated based on 25 m long clover like suspended-core ytterbium-doped fiber [64] or using a 18 m long polarization maintaining large mode area endlessly single mode PCF and a ytterbium-doped fiber laser as pump source [65].

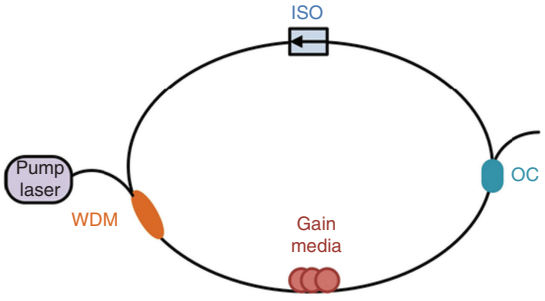

Figure 8 Example of a ring cavity fiber laser (OC - optical coupler and WDM – wavelength division multiplexer).

4.2 PCF for signal enhancement

The use of PCFs to enhance fiber ring laser signal is rather a popular technique. Several multiwavelength fiber lasers have been developed using PCFs for signal enhancement. A stable and broad bandwidth multiwavelength erbium-doped fiber ring laser was obtained using a highly nonlinear PCF and a Fabry-Perot filter [66]. Using a highly nonlinear PCF and a sample chirped fiber grating, a tunable and switchable multiwavelength erbium-doped fiber laser was accomplished [67]. A multiwavelength bismuth based erbium-doped fiber laser was achieved based on four-wave mixing effects in 100 m of a silica-core PCF [68]. By using a dual-core all-solid bandgap PCF a switchable multi-wavelength erbium-doped fiber laser was fabricated [69]. A tunable and switchable multi-wavelength erbium-doped fiber laser was accomplished by incorporating a highly nonlinear PCF in the ring cavity [70]. With a twin-core PCF a multiwavelength erbium-doped fiber laser was accomplished [71]. A multiwavelength source was demonstrated based on spectral splicing of supercontinuum light, generated on a PCF, using a FLM [72]. Multiwavelength fiber lasers were accomplished using four-wave mixing self-stability through a PCF [73, 74], based on previous theoretical studies [75]. Dual-wavelength erbium-doped fiber lasers were also accomplished with the assistance of a kind of PCF Robin Hood [76] and with 20 m highly nonlinear PCF [77]. A linearly polarized fiber laser was obtained using a short section of highly polarizing PCF [78], as depicted in Figure 9. Passive mode locking was also obtained in erbium-doped fiber ring lasers: using a highly nonlinear PCF with low and flat dispersion [79], or using a hollow-core PCF filled with few-layered grapheme oxide solution [80] or even through a solid-core highly nonlinear PCF [81]. Using a near-zero dispersion highly nonlinear PCF, a fiber laser with four types of pulses was obtained [82]. Some authors applied PCFs to the development of

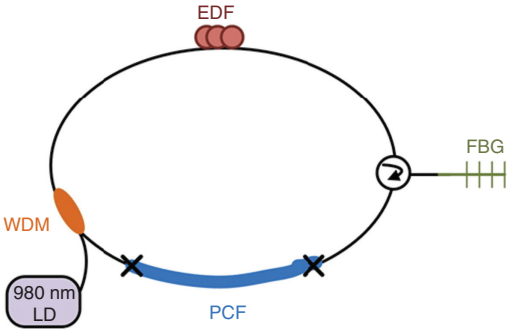

Figure 9 Schematic depiction of a fiber laser using a PCF for signal enhancement (LD – Laser Diode), adapted from [76].

Brillouin-erbium fiber lasers: using 20 m of polarization maintaining PCF [83], or using 20 m of PCF and 49 cm of bismuth-erbium-doped fiber [84], or even by using 20 m polarization maintaining PCF and 49 cm of bismuth-erbium-doped fiber [85]. Multiwavelength Brillouin-erbium fiber lasers were also demonstrated: using a 70 m solid-core highly nonlinear PCF [86, 87] or by using 100 m PCF [88]. Ytterbium-doped fiber lasers were developed: pumping a highly nonlinear PCF with zero-dispersion [89], or using a 20 m PCF to provide four-wave mixing [90], or through a polarization maintaining PCF for dispersion compensation [91], or even with an anomalous dispersion PCF [92]. Multiwavelength fiber ring lasers based on semiconductor optical amplifiers have been developed: using 100 m highly nonlinear PCF [93], or incorporating a PCF in order to improve the nonlinear polarization rotation effect [94], or even through a twin-core PCF based in-line comb filter [95].

4.3 PCF based loop mirrors

Several authors use photonic crystal fiber loop mirrors to obtain multiple wavelength peaks fiber lasers. Quite a lot multiwavelength erbium-doped fiber lasers were developed: based on a highly birefringent photonic crystal fiber (Hi-Bi PCF) FLM and a SMF FLM [96]; or through optical add-drop multiplexers and a Hi-Bi PCF loop mirror [97]; or using a PCF loop mirror and a sampled Hi-Bi FBG [98]; or by utilizing 25 m PCF in an figure-of-eight configuration [99]; or even by using a Hi-Bi PCF FLM and optical multiplexers to obtain multiple peaks in single-longitudinal mode operation [100]. A triple wavelength switchable erbium-doped fiber laser was accomplished through a highly non linear PCF [101]. Using a Hi-Bi PCF FLM a tunable single- and dual-wavelength erbium-doped fiber laser was obtained [102]. Using 25 m of highly nonlinear dispersion flattened PCF, an ultra short pulse fiber ring laser was fabricated [103]. A switchable multiwavelength Brillouin-erbium fiber laser was achieved using 100 m of PCF [104]. Using a PCF based figure-of-eight configuration, a multiwavelength Brillouin fiber laser was demonstrated [105]. A temperature-insensitive multiwavelength Raman fiber ring laser was obtained through a Hi-Bi PCF loop mirror [106]. And, even a semiconductor optical amplifier based multiwavelength fiber laser was accomplished incorporating a Hi-Bi PCF loop mirror [107].

4.4 Other PCF based ring fiber lasers

Other PCF based fiber lasers use, for example, Mach-Zehnder interferometers. Using a Mach-Zehnder interferometer filter based in splicing a section of few-mode photonic crystal fiber and two segments of SMF (been the air-holes on both sides of the PCF intentionally collapsed in the vicinity of the splices), a switchable multiwavelength fiber ring laser was accomplished [108]. A multiwavelength L-band fiber laser comb using a bismuth based erbium-doped fiber and 50 m photonic crystal fiber, was also demonstrated in a ring cavity configuration [109].

5 Linear cavity fiber lasers

Typical linear cavity fiber lasers entail two cavity ends to create a laser resonator. A simple technique to obtain a linear cavity resonator is to use highly reflective fiber ends at the opposite sides of the gain media, as depicted in Figure 10. In a linear cavity fiber laser the lasing wavelength will pass through the gain media twice per cycle, which makes it easier to reach deep saturation. Therefore, large tuning ranges as well as low threshold pump powers and high slope efficiencies can be easily achieved using this kind of cavity.

In this section of the manuscript, the developed linear cavity fiber lasers will be disclosed. Section 5.1 presents the developed lasers that use PCFs as the gain medium. The linear fiber lasers that employ PCFs for signal enhancement are described in Section 5.2. Section 5.3 describes the

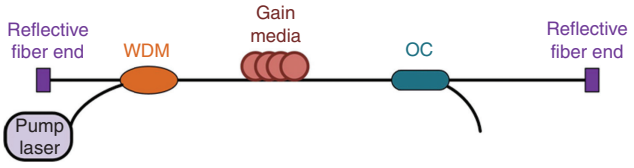

Figure 10 Example of a linear cavity fiber laser.

fiber lasers using fiber loop mirrors based on PCFs. And finally, other PCF based linear fiber lasers are presented in Section 5.4.

5.1 PCF as gain medium

A fiber laser is defined has a laser having an optical fiber as its gain medium. Some authors explored the possibility of using photonic crystal fibers as the gain media for their linear fiber lasers. PCFs have been used as Brillouin gain media: through using 25 m of a triangular solid-core PCF for microwave generation [110] and by employing 100 m of a triangular Ge-doped core PCF with low stimulated Brillouin scattering to obtain a tunable multiwavelength fiber laser [111]. These fibers have also been used to accomplish erbium-doped fiber lasers: using a 1.2 m erbium-doped solid core PCF between a FBG and a FLM [112], or by applying a liquid-filled erbium-doped suspended-core fiber between two FBGs [113], or even employing a erbium-doped hexagonal lattice PCF between a Sagnac loop mirror and a total reflector mirror [114]. Other authors were able to develop a high efficiency fiber laser by making use of a home-made double-cladding ytterbium-doped PCF [115].

5.2 PCF for signal enhancement

Due to photonic crystal fibers unique characteristics, several authors apply them in order to enhanced fiber laser's performances. The anomalous dispersion generated by a solid-core photonic crystal fiber was exploited in order to compensate the dispersion of a ytterbium fiber laser using a home-made fiber to obtain a stable mode-locked fiber laser [116] or used a solid-core photonic crystal fiber to achieve a supercontinuum Q-switched Yb fiber laser [117]. A triangular core highly nonlinear photonic crystal fiber was also utilized as a Brillouin gain medium, in order to enhance the performance of a multiwavelength erbium-doped fiber laser [118]. A direct end-of-the-fiber pulse delivery femtosecond ytterbium fiber laser was accomplished using a hollow-core polarization maintaining photonic crystal fiber to compress the laser output [119].

5.3 PCF based loop mirrors

Fiber loop reflectors fabricated solely with optical fibers are attractive and potentially useful components for applications in optical devices, such as fiber lasers or fiber sensors. Several multiwavelength Raman fiber lasers have been developed based in Hi-Bi PCF loop mirrors: in combination with cooperative Rayleigh scattering [120] or through using different combinations between two different Hi-Bi PCF FLMs and two different random mirrors [121]. Other multiwavelength Raman fiber laser were based in different PCFs: been a birefringent triangular solid-core PCF in a fiber loop mirror combined with a simple fiber loop reflector [122] or a suspended-core fiber loop mirror combined with a dual-random mirror [123]. There are, however, other multiwavelength fiber lasers for which the laser configuration is based in a fiber loop mirror structure: using a fiber loop mirror to accommodate an erbium-doped medium and a Hi-Bi PCF to obtain a multiwavelength erbium-doped fiber laser [124] or using a fiber loop mirror to accommodate Raman gain, multiple Rayleigh scattering and a Hi-Bi PCF in order to accomplish a double random mirror multiwavelength fiber laser [125]. A switchable dual-wavelength erbium-doped fiber laser was developed using a two-mode photonic crystal fiber loop mirror [126].

5.4 Other PCF based linear fiber lasers

PCFs have also been used as components of other fiber laser cavities. Using an erbium-doped aluminosilicate core photonic crystal fiber both as gain medium and as reflective mirror, by writing on it two FBGs, a fiber laser was accomplished [127]. An actively Q-switched erbium fiber laser was developed based in the combination of two FBGs and an active element, which was a polarization switch based on a microstructured fiber with electrically driven internal electrodes [128]. A multiwavelength Raman fiber laser was developed based in a random mirror in combination with a hybrid Fabry-Perot cavity, been the cavity fabricated through splicing a single mode fiber with a suspended-core fiber [129].

6 Sensing applications

Some of the all-fiber lasers developed find applications in the sensing field, been used simultaneously as sensors or only as illumination systems for sensing heads. A linear cavity Raman fiber laser based on a double random mirror, becomes a multiwavelength output laser when a suspended-core fiber loop mirror is added in the middle of the structure. When subjecting this suspended-core fiber loop mirror to displacement variations, the

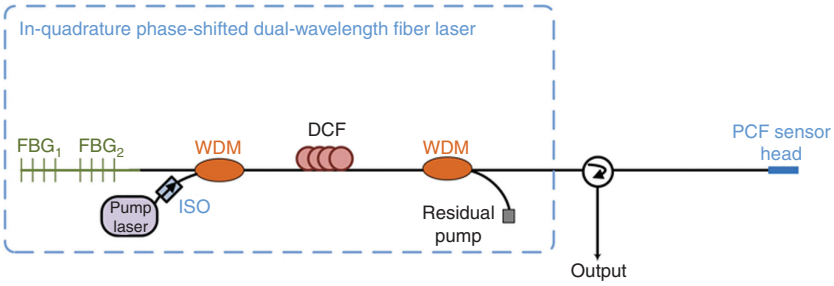

Figure 11 In-quadrature phase-shifted dual-wavelength fiber laser for PCF sensor head interrogation, adapted from [129].

multiwavelength structure presented a sensitivity of 0.011 dB/μm [123]. A linear multiwavelength Raman fiber laser developed based in a random mirror and a hybrid cavity (SMF and suspended-core fiber) was shown to present sensing capabilities since the hybrid cavity was sensible to temperature. This fiber laser was also a temperature sensor with a sensitivity of 6 pm/°C in a 200°C range [129]. A pulsed erbium ring fiber laser was developed based in an intracavity hollow-core PCF gas cell. This gas cell was filled with acetylene as the saturable absorber. Different operations were observed depending on the pressure in the gas cell: continuous wave operation at low pressures, Q-switching at intermediate pressures and mode locking at high pressures. In this paper the authors enhance the fact that the modes of operation depend on the density of the saturable absorber (gas), and as so this fiber laser may be explored for highly sensitive gas detection [130]. A home-made dual-wavelength Raman fiber laser was developed to generate two quadrature phase-sifted signals which would allow passive and accurate interrogation of a Fabry-Perot interferometric sensing cavity, as can be seen in Figure 11. This Fabry-Perot interferometric sensing cavity was fabricated by splicing a short length of a suspended-core fiber to a SMF. The use of this Raman fiber laser allowed proper temperature interrogation with a sensitivity of 0.84°/°C [131]. Also, a long range fiber sensor multiplexing network was developed based in a ring laser combining Raman and erbium-doped fiber amplification. In this structure, six suspended-core fiber loop mirror sensors were multiplexed remotely (up to 75 km) due to the high stability of the laser [132].

7 Conclusions

There is a diversity of all-fiber lasers based on photonic crystal fibers. Due to photonic crystal fiber's variety of features, they can be used in very distinctive ways in all-fiber lasers: as a gain medium, for signal enhancement and even as part of the cavity mirrors. Fiber ring lasers seem to be the more developed structures, but linear cavity fiber lasers also present a remarkable number of developed configurations. The overall assessment of all-fiber lasers based on photonic crystal fiber is presented, showing their valuable contribution in the sensing field.

Acknowledgments: The authors are grateful to the Spanish government project TEC2010-20224-C02-01 and the European project ECOAL-MGT – SUDOE Program.

Received June 26, 2013; accepted November 7, 2013

References

[1] Gordon JP, Zeiger HJ, Townes CH. Molecular microwave oscillator and new hyperfine structure in the microwave spectrum of Nh3. Phys Rev 1954;95:282–4.
[2] Schawlow AL, Townes CH. Infrared and optical masers. Phys Rev 1958;112:1940–9.
[3] Maiman TH. Stimulated optical radiation in ruby. Nature 1960;187:493–4.
[4] Hecht J. Short history of laser development. Opt Eng 2010;49: 091002-1–23.
[5] Snitzer E, Osterberg H. Observed dielectric waveguide modes in visible spectrum. J Opt Soc Am 1961;51:499–505.
[6] Snitzer E. Proposed fiber cavities for optical masers. J Appl Phys 1961;32:36–9.
[7] Koester CJ, Snitzer E. Amplification in fiber laser. Appl Optics 1964;3:1182–6.
[8] Mears RJ, Reekie L, Poole SB, Payne DN. Neodymium-doped silica single-mode fiber lasers. Electron Lett 1985;21: 738–40.
[9] Reekie L, Mears RJ, Poole SB, Payne DN. Tunable single-mode fiber lasers. J Lightwave Technol 1986;4:956–60.
[10] Russell P. Photonic crystal fibers. Science 2003;299: 358–62.

[11] Laurent Bigot PR, Roy P. Fibres à cristal photonique: 10 ans d'existence et un vaste champ d'applications. Images de la physique 2007;71–80.
[12] Cerqueira SA. Recent progress and novel applications of photonic crystal fibers. Rep Prog Phys 2010;73:024401.
[13] Knight JC, Birks TA, Russell PS, Atkin DM. All-silica single-mode optical fiber with photonic crystal cladding. Opt Lett 1996;21:1547–9.
[14] Birks TA, Knight JC, Russell PS. Endlessly single-mode photonic crystal fiber. Opt Lett 1997;22:961–3.
[15] Mogilevtsev D, Birks TA, Russell PS. Group-velocity dispersion in photonic crystal fibers. Opt Lett 1998;23:1662–4.
[16] Knight JC, Arriaga J, Birks TA, Ortigosa-Blanch A, Wadsworth WJ, Russell PS. Anomalous dispersion in photonic crystal fiber. IEEE Photonic Tech L 2000;12:807–9.
[17] Ortigosa-Blanch A, Knight JC, Wadsworth WJ, Arriaga J, Mangan BJ, Birks TA, Russell PSJ. Highly birefringent photonic crystal fibers. Opt Lett 2000;25:1325–7.
[18] Cregan RF, Mangan BJ, Knight JC, Birks TA, Russell PS, Roberts PJ, Allan DC. Single-mode photonic band gap guidance of light in air. Science 1999;285:1537–9.
[19] Couny F, Benabid F, Light PS. Large-pitch kagome-structured hollow-core photonic crystal fiber. Opt Lett 2006;31:3574–6.
[20] Benabid F, Knight JC, Antonopoulos G, Russell PSJ. Stimulated Raman scattering in hydrogen-filled hollow-core photonic crystal fiber. Science 2002;298:399–402.
[21] Mortensen NA, Folkenberg JR, Nielsen MD, Hansen KP. Modal cutoff and the V parameter in photonic crystal fibers. Opt Lett 2003;28:1879–81.
[22] Humbert G, Wadsworth WJ, Leon-Saval SG, Knight JC, Birks TA, Russell PSJ, Lederer MJ, Kopf D, Wiesauer K, Breuer EI, Stifter D. Supercontinuum generation system for optical coherence tomography based on tapered photonic crystal fibre. Opt Express 2006;14:1596–603.
[23] Holzwarth R, Udem T, Hansch TW, Knight JC, Wadsworth WJ, Russell PSJ. Optical frequency synthesizer for precision spectroscopy. Phys Rev Lett 2000;85:2264–7.
[24] Pinto AMR, Lopez-Amo M. Photonic crystal fibers for sensing applications. J Sensors 2012;2012:21.
[25] Frazao O, Baptista JM, Santos JL, Roy P. Curvature sensor using a highly birefringent photonic crystal fiber with two asymmetric hole regions in a Sagnac interferometer. Appl Opt 2008;47:2520–3.
[26] Zhang H, Liu B, Wang Z, Luo JH, Wang SX, Jia CH, Ma XR. Temperature-insensitive displacement sensor based on high-birefringence photonic crystal fiber loop mirror. Opt Appl 2010;40:209–17.
[27] Mathews S, Farrell G, Semenova Y. Liquid crystal infiltrated photonic crystal fibers for electric field intensity measurements. Appl Opt 2011;50:2628–35.
[28] Thakur HV, Nalawade SM, Gupta S, Kitture R, Kale SN. Photonic crystal fiber injected with Fe(3)O(4) nanofluid for magnetic field detection. Appl Phys Lett 2011;99:161101.
[29] Fu HY, Wu C, Tse MLV, Zhang L, Cheng KCD, Tam HY, Guan BO, Lu C. High pressure sensor based on photonic crystal fiber for downhole application. Appl Optics 2010;49:2639–43.
[30] Qian WW, Zhao CL, He SL, Dong XY, Zhang SQ, Zhang ZX, Jin SZ, Guo JT, Wei HF. High-sensitivity temperature sensor based on an alcohol-filled photonic crystal fiber loop mirror. Opt Lett 2011;36:1548–50.
[31] Zu P, Chan CC, Jin YX, Gong TX, Zhang YF, Chen LH, Dong XY. A Temperature-insensitive twist sensor by using low-birefringence photonic-crystal-fiber-based Sagnac interferometer. IEEE Photonic Tech L 2011;23:920–2.
[32] Fan CF, Chiang CL, Yu CP. Birefringent photonic crystal fiber coils and their application to transverse displacement sensing. Opt Express 2011;19:19948–54.
[33] Silva S, Santos JL, Malcata FX, Kobelke J, Schuster K, Frazao O. Optical refractometer based on large-core air-clad photonic crystal fibers. Opt Lett 2011;36:852–4.
[34] Thakur HV, Nalawade SM, Saxena Y, Grattan KTV. All-fiber embedded PM-PCF vibration sensor for Structural Health Monitoring of composite. Sensor Actuat a-Phys 2011;167:204–12.
[35] Ritari T, Tuominen J, Ludvigsen H, Petersen JC, Sorensen T, Hansen TP, Simonsen HR. Gas sensing using air-guiding photonic bandgap fibers. Opt Express 2004;12:4080–7.
[36] Coscelli E, Sozzi M, Poli F, Passaro D, Cucinotta A, Selleri S, Corradini R, Marchelli R. Toward a highly specific DNA biosensor: PNA-modified suspended-core photonic crystal fibers. IEEE J Sel Top Quant Elec 2010;16:967–72.
[37] Ruan YL, Schartner EP, Ebendorff-Heidepriem H, Hoffmann P, Monro TM. Detection of quantum-dot labeled proteins using soft glass microstructured optical fibers. Opt Express 2007;15:17819–26.
[38] Yan H, Liu J, Yang CX, Jin GF, Gu C, Hou L. Novel index-guided photonic crystal fiber surface-enhanced Raman scattering probe. Opt Express 2008;16:8300–5.
[39] Wu C, Guan B-O, Lu C, Tam H-Y. Salinity sensor based on polyimide-coated photonic crystal fiber. Opt Express 2011;19:20003–8.
[40] Yang XH, Wang LL. Fluorescence pH probe based on microstructured polymer optical fiber. Opt Express 2007;15:16478–83.
[41] Mathew J, Semenova Y, Rajan G, Farrell G. Humidity sensor based on photonic crystal fibre interferometer. Electron Lett 2010;46:1341–3.
[42] Russell PSJ. Photonic-crystal fibers. J Lightwave Technol 2006;24:4729–49.
[43] Euser TG, Garbos MK, Chen JSY, Russell PS. Precise balancing of viscous and radiation forces on a particle in liquid-filled photonic bandgap fiber. Opt Lett 2009;34:3674–6.
[44] Schmidt M, Cubillas AM, Taccardi N, Euser TG, Cremer T, Maier F, Steinruck HP, Russell PS, Wasserscheid P, Etzold BJM. Chemical and (photo)-catalytical transformations in photonic crystal fibers. Chemcatchem 2013;5:641–50.
[45] Duval A, Lhoutellier M, Jensen JB, Hoiby PE, Missier V, Pedersen LH, Hansen TP, Bjarklev A, Bang O. Photonic crystal fiber based antibody detection. P IEEE Sensor 2004;1–3:1222–5.
[46] Magalhaes F, Carvalho JP, Ferreira LA, Araujo FM, Santos JL. Methane detection system based on Wavelength Modulation Spectroscopy and hollow-core fibres. Sensors 2008 IEEE 2008:1277–80.
[47] Pinto A, Baptista J, Santos J, Lopez-Amo M, Frazão O. Micro-displacement sensor based on a hollow-core photonic crystal fiber. Sensors-Basel 2012;12:17497–503.
[48] Wiersma DS. The physics and applications of random lasers. Nat Phys 2008;4:359–67.
[49] Agrawal CHGP. Raman Amplification in Fiber Optical Communication Systems, Optics and Photonics. London: Elsevier Academic Press, 2005.

[50] Mortimore DB. Fiber loop reflectors. IEEE J Lightwave Technol 1988;6:1217–24.
[51] Agrawal GP. Applications of Nonlinear Fiber Optics, 2nd ed. Boston: Elsevier, Amsterdam, 2008:xiv, 508.
[52] Zhang AL, Demokan MS, Tam HY. Room temperature multiwavelength Erbium-doped fiber ring laser using a highly nonlinear photonic crystal fiber. Opt Commun 2006;260:670–4.
[53] Liu XM, Zhou XQ, Tang XF, Ng J, Hao JZ, Chai TY, Leong E, Lu C. Switchable and tunable multiwavelength Erbium-doped fiber laser with fiber bragg gratings and photonic crystal fiber. IEEE Photonic Tech L 2005;17:1626–8.
[54] Feng XH, Tam HY, Wai PKA. Switchable multiwavelength Erbium-doped fiber laser with a multimode fiber Bragg grating and photonic crystal fiber. IEEE Photonic Tech L 2006;18: 1088–90.
[55] Chen WG, Lou SQ, Wang LW, Zou H, Lu WL, Jian SS. Switchable multi-wavelength fiber ring laser using a side-leakage photonic crystal fiber based filter. Opt Laser Technol 2012;44:611–6.
[56] Yang XF, Dong XY, Zhang SM, Lu FY, Zhou XQ, Lu C. Multiwavelength Erbium-doped fiber laser with 0.8-nm spacing using sampled Bragg grating and photonic crystal fiber. IEEE Photonic Tech L 2005;17:2538–40.
[57] Zheng W, Ruan S, Zhang M, Liu W, Zhang Y, Yang X. Switchable multi-wavelength Erbium-doped photonic crystal fiber laser based on nonlinear polarization rotation. Opt Laser Technol 2013;50:145–9.
[58] Liu XM, Yang XF, Lu FY, Ng JH, Zhou XQ, Lu C. Stable and uniform dual-wavelength Erbium-doped fiber laser based on fiber Bragg gratings and photonic crystal fiber. Opt Express 2005;13:142–7.
[59] Yang XF, Lu FY, Dong XY, Li ZH, Zhou XQ, Lu C. Four-wave-mixing-assisted room-temperature four-wavelength Erbium-doped fiber lasers. Opt Eng 2006;45:064202-1–4.
[60] Zhang AL. Suppression of multiple mode instabilities in an Erbium-doped fiber laser by inserting a highly nonlinear photonic crystal fiber. Microw Opt Techn Let 2011;53: 1564–6.
[61] Sanchez-Martin JA, Rebolledo MA, Alvarez JM, Berdejo V, Diez A, Andres MV. Erbium-doped photonic crystal fiber lasers optimization by microstructure control: experimental study analysis. Appl Phys B-Lasers O 2013;110:579–84.
[62] Ahmad H, Parvizi R, Shahabuddin NS, Yusoff Z, Harun SW. Effect of gain medium on the performance of brillouin fiber laser. Microw Opt Techn Let 2010;52:2158–60.
[63] Tow KH, Leguillon Y, Fresnel S, Besnard P, Brilland L, Mechin D, Toupin P, Troles J. Toward more coherent sources using a microstructured chalcogenide brillouin fiber laser. IEEE Photonic Tech L 2013;25:238–41.
[64] Chamorovskiy A, Chamorovskiy Y, Vorob'ev I, Okhotnikov OG. 95-Femtosecond suspended core ytterbium fiber laser. IEEE Photonic Tech L 2010;22:1321–3.
[65] Zlobina EA, Kablukov SI, Babin SA. Tunable CW all-fiber optical parametric oscillator operating below 1 mu m. Opt Express 2013;21:6777–82.
[66] Zhang AL, Liu HL, Demokan MS, Tam HY. Stable and broad bandwidth multiwavelength fiber ring laser incorporating a highly nonlinear photonic crystal fiber. IEEE Photonic Tech L 2005;17:2535–7.
[67] Liu XM, Chung Y, Lin A, Zhao W, Lu KQ, Wang YS, Zhang TY. Tunable and switchable multi-wavelength Erbium-doped fiber laser with highly nonlinear photonic crystal fiber and polarization controllers. Laser Phys Lett 2008;5:904–7.
[68] Parvizi R, Harun SW, Shahabuddin NS, Yusoff Z, Ahmad H. Multi-wavelength bismuth-based Erbium-doped fiber laser based on four-wave mixing effect in photonic crystal fiber. Opt Laser Technol 2010;42:1250–2.
[69] Zhao J, Wang Z, Liu Y, Liu B. Switchable-multi-wavelength fiber laser based on dual-core all-solid photonic bandgap fiber. Front Optoelectron China 2010;3:283–8.
[70] Cheng JQ, Ruan SC. Tunable and switchable multi-wavelength Erbium-doped photonic crystal fiber ring laser incorporating a length of highly nonlinear photonic crystal fiber. Opt Commun 2011;284:5185–8.
[71] Kim BK, Chung Y. Multiwavelength Erbium-doped fiber laser using twin-core photonic crystal fiber. Laser Phys 2012;22:967–71.
[72] Shahabuddin NS, Mohamad H, Mahdi MA, Yusoff Z, Ahmad H, Harun SW. Broad spectral sliced multiwavelength source with a mode locked fiber laser. Laser Phys 2012;22:212–5.
[73] Liu XM, Zhao W, Zhang TY, Lu KQ, Sun CD, Wang YS, Ouyang X, Hou X, Chen GF. Multi-wavelength Erbium-doped fibre lasers on assistance of high-nonlinear photonic-crystal fibres. Chinese Phys Lett 2006;23:1787–9.
[74] Liu XM. Four-wave mixing self-stability based on photonic crystal fiber and its applications on Erbium-doped fiber lasers. Opt Commun 2006;260:554–9.
[75] Liu XM, Lu C. Self-stabilizing effect of four-wave mixing and its applications on multiwavelength Erbium-doped fiber lasers. IEEE Photonic Tech L 2005;17:2541–3.
[76] Liu XM, Zhao W, Lu KQ, Zhang TY, Sun CD, Wang YS, Hou X, Chen GF. Room-temperature dual-wavelength Erbium-doped fibre laser based on a sampled fibre Bragg grating and a photonic Robin Hood. J Mod Optic 2006;53:2785–92.
[77] Jin L, Kai G-y, Xu L-l, Liu B, Zhang J, Liu Y-g, Yuan S-z, Dong X-y. Switchable dual-wavelength Erbium-doped fiber laser with a tilted fiber grating. Optoelectron Lett 2007;3:27–9.
[78] Delgado-Pinar M, Diez A, Cruz JL, Andres MV. Linearly polarized all-fiber laser using a short section of highly polarizing microstructured fiber. Laser Phys Lett 2008;5: 135–8.
[79] Zhang SM, Lu FY, Dong XY, Shum P, Yang XF, Zhou XQ, Gong YD, Lu C. Passive mode locking at harmonics of the free spectral range of the intracavity filter in a fiber ring laser. Opt Lett 2005;30:2852–4.
[80] Liu ZB, He XY, Wang DN. Passively mode-locked fiber laser based on a hollow-core photonic crystal fiber filled with few-layered graphene oxide solution. Opt Lett 2011;36:3024–6.
[81] Kang MS, Joly NY, Russell PSJ. Passive mode-locking of fiber ring laser at the 337th harmonic using gigahertz acoustic core resonances. Opt Lett 2013;38:561–3.
[82] Wang LR, Liu XM, Gong YK, Mao D, Duan LN. Observations of four types of pulses in a fiber laser with large net-normal dispersion. Opt Express 2011;19:7616–24.
[83] Shahi S, Harun SW, Dimyati K, Ahmad H. Brillouin fiber laser with significantly reduced gain medium length operating in l-band region. Prog Electromagnetics Res Lett 2009; 8:143–9.

[84] Harun SW, Shahi S, Ahmad H. Brillouin fiber laser with a 49 cm long Bismuth-based Erbium-doped fiber. Laser Phys Lett 2010;7:60–2.
[85] Harun SW, Aziz SN, Tamchek N, Shahabuddin NS, Ahmad H. Brillouin fibre laser with 20 m-long photonic crystal fibre. Electron Lett 2008;44:1065–66.
[86] Li Y, Liu YG, Xu JB, Tai BY, Wang Z. Tunable multiwavelength brillouin-erbium ring-cavity fiber laser with short-length photonic crystal fiber. Laser Phys 2010;20:528–32.
[87] Zhao JF, Yang XF, Tong ZR, Liu YG, Zhao QD. Simple tunable multiwavelength Brillouin/Erbium fiber laser utilizing short-length photonic crystal fiber. Optik 2011;122: 1046–9.
[88] Shahabuddin NS, Ahmad H, Othman M, Ali S, Yusoff Z, Harun SW. An efficient photonic crystal fiber-based brillouin erbium fiber laser using a fiber bragg grating for multi-wavelength generation. Fiber Integrated Opt 2011;30: 259–64.
[89] Rulkov AB, Vyatkin MY, Popov SV, Taylor JR, Gapontsev VP. High brightness picosecond all-fiber generation in 525–1800 nm range with picosecond Yb pumping. Opt Express 2005;13: 377–81.
[90] Shahabuddin NS, Ismail MA, Paul MC, Damanhuri SSA, Harun SW, Ahmad H, Pal M, Bhadra SK. Multi-wavelength ytterbium doped fiber laser based on longitudinal mode interference. Laser Phys 2012;22:252–5.
[91] Sumimura K, Yoshida H, Tanaka K, Okada H, Fujita H, Nakatsuka M, Sawada H, Yoshida M. All polarization-maintaining type Yb mode-locked fiber laser with photonic crystal fiber. Electron Comm Jpn 2 2007;90:27–32.
[92] Zhang ZX, Senel C, Hamid R, Ilday FO. Sub-50 fs Yb-doped laser with anomalous-dispersion photonic crystal fiber. Opt Lett 2013;38:956–8.
[93] Harun SW, Parvizi R, Shahabuddin NS, Yusoff Z, Ahmad H. Semiconductor optical amplifier-based multi-wavelength ring laser utilizing photonic crystal fiber. J Mod Optic 2010;57: 637–40.
[94] Shahabuddin NS, Tan SJ, Ismail MA, Ahmad H, Yusoff Z, Harun SW. Multi-wavelength fiber laser based on nonlinear polarization rotation in semiconductor optical amplifier and photonic crystal fiber. Laser Phys 2012;22:1257–9.
[95] Kim BK, Chung Y. Tunable and switchable SOA-based multi-wavelength fiber laser using twin-core photonic crystal fiber. Laser Phys Lett 2012;9:734–8.
[96] Liu ZY, Liu YG, Du JB, Kai GY, Dong XY. Tunable multiwavelength Erbium-doped fiber laser with a polarization-maintaining photonic crystal fiber Sagnac loop filter. Laser Phys Lett 2008;5:446–8.
[97] Rota-Rodrigo S, Perez-Herrera RA, Ibanez I, Pinto AMR, Fernandez-Vallejo M, Lopez-Amo M. Multiwavelength fiber ring laser based on optical add-drop multiplexers and a photonic crystal fiber Sagnac interferometer. Opt Laser Technol 2013;48:72–4.
[98] Liu ZY, Liu YG, Du JB, Yuan SZ, Dong XY. Channel-spacing and wavelength switchable multiwavelength Erbium-doped fiber laser using sampled Hi-Bi fiber grating and photonic crystal fiber loop mirror. Laser Phys Lett 2008;5:122–5.
[99] Chen D. Stable multi-wavelength Erbium-doped fiber laser based on a photonic crystal fiber Sagnac loop filter. Laser Phys Lett 2007;4:437–9.
[100] Rota-Rodrigo S, Ibanez I, Lopez-Amo M. Multi-wavelength fiber laser in single-longitudinal mode operation using a photonic crystal fiber Sagnac interferometer. Appl Phys B-Lasers O 2013;110:303–8.
[101] Han YG. Triple-wavelength switchable multiwavelength Erbium-doped fiber laser based on a highly nonlinear photonic crystal fiber. J Korean Phys Soc 2010;56:1251–5.
[102] Im JE, Kim BK, Chung Y. Tunable single- and dual-wavelength Erbium-doped fiber laser based on Sagnac filter with a high-birefringence photonic crystal fiber. Laser Phys 2011;21: 540–7.
[103] Ma SZ, Li WB, Hu HY, Dutta NK. High speed ultra short pulse fiber ring laser using photonic crystal fiber nonlinear optical loop mirror. Opt Commun 2012;285:2832–5.
[104] Shahabuddin NS, Ahmad H, Yusoff Z, Harun SW. Spacing-switchable multiwavelength fiber laser based on nonlinear polarization rotation and brillouin scattering in photonic crystal fiber. IEEE Photonics J 2012;4:34–8.
[105] Parvizi R, Arof H, Ali NM, Ahmad H, Harun SW. 0.16 nm spaced multi-wavelength Brillouin fiber laser in a figure-of-eight configuration. Opt Laser Technol 2011;43:866–9.
[106] Han YG. Temperature-insensitive multiwavelength raman fiber ring laser with high tunability based on a polarization-maintaining photonic-crystal fiber. J Korean Phys Soc 2009;55:1205–9.
[107] Im JE, Kim BK, Chung Y. Stable SOA-based multi-wavelength fiber ring laser using Sagnac loop mirror incorporating a high-birefringence photonic crystal fiber. Laser Phys 2010;20:1918–22.
[108] Chen WG, Lou SQ, Feng SC, Wang LW, Li HL, Guo TY, Jian SS. Switchable multi-wavelength fiber ring laser based on a compact in-fiber Mach-Zehnder interferometer with photonic crystal fiber. Laser Phys 2009;19:2115–9.
[109] Salem AMR, Al-Mansoori MH, Hizam H, Noor SBM, Abu Bakar MH, Mahdi MA. Multiwavelength L-band fiber laser with bismuth-oxide EDF and photonic crystal fiber. Appl Phys B-Lasers O 2011;103:363–8.
[110] Geng D, Yang DX, Zhang XM, Dong QJ, Wang L, Shao XJ. All-optical generation of microwave using a photonic crystal fiber Brillouin laser based on Bragg grating Fabry-Perot cavity. Microw Opt Techn Let 2008;50:809–14.
[111] Nasir MNM, Yusoff Z, Al-Mansoori MH, Rashid HAA, Choudhury PK. Widely tunable multi-wavelength Brillouin-erbium fiber laser utilizing low SBS threshold photonic crystal fiber. Opt Express 2009;17:12829–34.
[112] Yang HL, Ruan SC, Yu YQ, Zhou H. Erbium-doped photonic crystal fiber laser with 49 mW. Opt Commun 2010;283: 3176–9.
[113] Guzman-Chavez AD, Diez A, Cruz JL, Andres MV. An experimental investigation on the transient characteristics of a liquid-filled Erbium-doped Y-shaped microstructured optical fiber similar to. Laser Phys 2012;22:579–83.
[114] Zheng WJ, Cheng JQ, Ruan SC, Zhang M, Liu WL, Yang X, Zhang YY. A Switchable multi-wavelength erbium-doped photonic crystal fiber laser with linear cavity configuration. Chinese Phys Lett 2012;29:124204-1–3.
[115] Chen W, Li JY, Lu PX, Li SY, Ji LL, Jiang ZW, Zhang JH, Peng JG. All-fibre ytterbium-doped photonic crystal fibre laser with high efficiency. Chinese Phys Lett 2008;25: 960–2.

[116] Herda R, Kivisto S, Okhotnikov OG, Kosolapov AF, Levchenko AE, Semjonov SL, Dianov EM. Environmentally stable mode-locked fiber laser with dispersion compensation by index-guided photonic crystal fiber. IEEE Photonic Tech L 2008;20:217–9.
[117] Cascante-Vindas J, Diez A, Cruz JL, Andres MV. Supercontinuum Q-switched Yb fiber laser using an intracavity microstructured fiber. Opt Lett 2009;34:3628–30.
[118] Nasir MNM, Yusoff Z, Mansoori MHA, Rashid HAA, Choudhury PK. On the pre-amplified linear cavity multi-wavelength brillioun-erbium fiber laser with low SBS threshold highly nonlinear photonic crystal fiber. Laser Phys 2009;19: 2027–30.
[119] Turchinovich D, Liu XM, Laegsgaard J. Monolithic all-PM femtosecond Yb-fiber laser stabilized with a narrow-band fiber Bragg grating and pulse-compressed in a hollow-core photonic crystal fiber. Opt Express 2008;16:14004–14.
[120] Pinto AMR, Frazao O, Santos JL, Lopez-Amo M. Multiwavelength fiber laser based on a photonic crystal fiber loop mirror with cooperative Rayleigh scattering. Appl Phys B-Lasers O 2010;99:391–5.
[121] Pinto AMR, Frazao O, Santos JL, Lopez-Amo M. Multiwavelength Raman fiber lasers using Hi-Bi photonic crystal fiber loop mirrors combined with random cavities. J Lightwave Technol 2011;29:1482–8.
[122] Chen DR, Qin S, Shen LF, Chi H, He SL. An all-fiber multi-wavelength Raman laser based on a PCF Sagnac loop filter. Microw Opt Techn Let 2006;48:2416–8.
[123] Pinto AMR, Bravo M, Fernandez-Vallejo M, Lopez-Amo M, Kobelke J, Schuster K. Suspended-core fiber Sagnac combined dual-random mirror Raman fiber laser. Opt Express 2011;19:11906–15.
[124] Yu X, Liu D, Dong H, Fu S, Dong X, Tang M, Shum P, Ngo NQ. Temperature stability improvement of a multiwavelength Sagnac loop fiber laser using a high-birefringent photonic crystal fiber as a birefringent component. Opt Eng 2006;45:044201.
[125] Pinto AMR, Lopez-Amo M. Double random mirror Hi-Bi photonic crystal fiber Sagnac based multiwavelength fiber laser. Appl Phys B: Lasers Optics 2011;103:771–5.
[126] Chen W-g, Lou S-q, Wang L-w, Li H-l, Guo T, Jian S-s. Switchable dual-wavelength Erbium-doped fiber laser based on the photonic crystal fiber loop mirror and chirped fiber Bragg grating. Optoelectron Lett 2010;6:94–7.
[127] Canning J, Groothoff N, Buckley E, Ryan T, Lyytikainen K, Digweed J. All-fibre photonic crystal distributed Bragg reflector (PC-DBR) fibre laser. Opt Express 2003;11:1995–2000.
[128] Yu ZW, Malmstrom M, Tarasenko O, Margulis W, Laurell F. Actively Q-switched all-fiber laser with an electrically controlled microstructured fiber. Opt Express 2010;18:11052–7.
[129] Pinto AMR, Lopez-Amo M, Kobelke J, Schuster K. Temperature fiber laser sensor based on a hybrid cavity and a random mirror. J Lightwave Technol 2012;30:1168–72.
[130] Marty PT, Morel J, Feurer T. Pulsed erbium fiber laser with an acetylene-filled photonic crystal fiber for saturable absorption. Opt Lett 2011;36:3569–71.
[131] Pinto AMR, Frazao O, Santos JL, Lopez-Amo M, Kobelke J, Schuster K. Interrogation of a suspended-core fabry-perot temperature sensor through a dual wavelength Raman fiber laser. J Lightwave Technol 2010;28:3149–55.
[132] Bravo M, Fernandez-Vallejo M, Echapare M, Lopez-Amo M, Kobelke J, Schuster K. Multiplexing of six micro-displacement suspended-core Sagnac interferometer sensors with a Raman-Erbium fiber laser. Opt Express 2013;21:2971–7.

Ana M.R. Pinto was born in Porto, Portugal, in 1982. In 2006, she received the Physics degree from Universidade do Minho, Portugal. She also received the Communications Technology Master and PhD from Universidad Pública de Navarra, Spain in 2009 and 2012, respectively. From 2007 to 2008, she was with the Optoelectronics and Electronic Systems Unit of InescPorto (Portugal) working with a research grant. In the PhD scope, she has done a research period in 2011 at the Russell's Division in the Max-Planck Institute for the Science of Light and in 2012 at the Optoelectronics and Electronic Systems Unit of InescPorto (Portugal). Her present research interests include photonic crystal fibers, fiber optic sensing and optical communications.

Manuel López-Amo received the telecommunications M.Eng and Ph.D. degrees from the Universidad Politécnica de Madrid, Spain in 1985 and 1989, respectively. From 1985 to 1996, he belonged to the Photonic Technology Department of the Universidad Politécnica de Madrid, where in 1990 he became an Associate Professor. In 1996, he moved to Public University of Navarra (Pamplona, Spain) where he became a Full Professor in the Electrical and Electronic Engineering department and is currently the head of the optical communications group of this department. He has been Chairman of the Optoelectronic Committee of Spain. He has been the leader of more than 30 research projects and he has coauthored more than 200 works in international refereed journals and conferences related with fiber-optic networks, fiber-optic amplifiers and lasers, fiber-optic sensors, and integrated optics. He is a member of the technical committees of the International Conference on fiber optic sensors (OFS), the European Workshop on optical fiber sensors (EWOFS), and European cost TD1001 action, among others. Professor López-Amo is senior member of the IEEE and member of the OSA.